ISIJ International, Vol. 50 (2010), No. 11, pp. 1707–1712

Liquid Iron Wetting of Calcium Aluminates

Brian J. MONAGHAN,[1)] Michael W. CHAPMAN[2)] and Sharon A. NIGHTINGALE[1)]

1) PYROmetallurgical Research Group, University of Wollongong, NSW 2522 Australia. 2) Formally a Post Graduate Student of the University of Wollongong. Now at BlueScope Steel Limited, P.O. Box 202, Port Kembla, NSW 2505 Australia.

(*Received on July 1, 2010; accepted on July 20, 2010*)

An investigation has been carried out to assess the wetting behaviour of liquid iron carbon alloys on alumina, CA6 ($CaO \cdot 6Al_2O_3$), CA2 ($CaO \cdot 2Al_2O_3$) and CA ($CaO \cdot Al_2O_3$). The melt compositions studied were 2 and 5 mass% [C] over a temperature range of 1 450 to 1 550°C. It was found that the systems studied were in general non-wetting, and that the contact angle dropped from approximately 140° to 110° as the calcium content of the substrates increased. The data for alumina were in good agreement with the literature. These data have been used to assess whether capillary phenomena play a significant role in coke dissolution in liquid iron. In previous studies it was found that as coke dissolved, a mineral layer consisting of alumina and calcium aluminates formed at the coke iron interface and that as time passed the mineralogy of the layer changed from CA6 to CA2 to CA. The rate of coke dissolution slowed considerably with the occurrence of the CA phase. It was not clear whether this was solely a densification effect, or if a capillary wetting issue was contributing to a reduction of the contact area. The contact angle measurements of iron on alumina, CA6, CA2 and CA have been discussed in light of this coke dissolution study, and a simple capillary penetration model used to assess the wetting effects. It was found that the change of wetting associated with the calcium enrichment of the mineral layer did not have a significant effect on the rate of coke dissolution.

KEY WORDS: wetting; calcium aluminates; coke dissolution; ironmaking.

1. Introduction

Coke is a key material in the iron blast furnace and many other metallurgical processes. Understanding its reaction behaviour is critical if these processes are to be optimised with respect to their carbon/coke usage.[1)] Recent studies focussed on mineral layer development as coke dissolves in liquid iron have resulted in new information on how the layer grows, evolves and effects carbon dissolution rates.[2–4)] In these studies it was found that the composition and morphology of the mineral layer formed on dissolution had a profound effect on the kinetics of reaction. Moreover it was found that the layer was primarily calcium aluminate based and that over time (0–120 min) became progressively enriched with calcium. The minerals identified in the layer were alumina, CA6, CA2, and CA. The appearance of the CA phase coincided with a significant decrease in the rate of carbon transfer to iron. The CA phase is a dense block-like structure and its appearance caused a densification of the mineral layer. The CA6 and CA2 formed relatively porous structures. Specific details of the minerals structures are given in **Table 1**.[5,6)]

It was argued[2,4)] that this densification due to the change in mineral structure caused the decrease in the coke dissolution kinetics. On the basis of rate constant plots corrected for thermodynamic driving force effects, the coke dissolution kinetics was characterised as a two stage process. In stage I, the coke dissolution was fast and, at least in part as, a result of good contact between the liquid iron and coke due to the porous nature of the mineral layer (CA6 and CA2) formed. In stage II the appearance of a denser CA layer formed reduced the contact between the coke and liquid iron slowing the kinetics. These findings were broadly consistent with what had been previously reported in the literature[7–13)] but the information on the mineral structures formed was new.

Table 1. Structure and melting points of the identified calcium aluminates.

Phase	Abbreviation	Typical Structure [5)]	Melting Point [6)]
$CaO.6Al_2O_3$	CA6	Acicular needles	1830°C
$CaO.2Al_2O_3$	CA2	Plate like crystals / Needles	1762°C
$CaO.Al_2O_3$	CA	Dense fine grains	1602°C

Carbon transfer resulting from coke dissolving in iron can be represented by the following equation where [C] denotes solution in iron.

$$C_{coke} = [C] \quad \text{.....(1)}$$

A simple schematic of this dissolution process is given in **Fig. 1**, where Fig. 1(a) represents a persistent mineral (ash) layer formed as the coke dissolves in liquid iron. The channels represent a necessary transfer path if significant coke (carbon) dissolution is to be maintained after layer formation. It is assumed here that the mineral layer is solid, as was the case in the previous studies by Chapman and Monaghan,[2,4)] but this would be at least in part dependant on the

© 2010 ISIJ

specific mineral components of the cokes used. Figs. 1(b) and 1(c) should be considered relative to Fig. 1(a) and represent possible explanations why the rate of coke dissolution slowed. In Fig. 1(b) a reduction in contact area is being considered as result of the denser CA phase evolving reducing either the number or radius of the channels. In Fig. 1(c) the possibility being considered is a gap appearing as a result of either capillary forces restricting iron coke contact or gas formation due to side reactions in the coke–mineral layer–iron area. An example is possible reduction of silica in the ash layer with carbon in the coke or iron. This could be represented by the following equation

$$\langle SiO_2 \rangle + 2\langle C \rangle = 2(CO) + [Si] \quad \text{.....(2)}$$

or

$$\langle SiO_2 \rangle + 2(CO) = 2(CO_2) + [Si] \quad \text{.....(3)}$$

where brackets indicate ⟨solid⟩, (gas) and [in solution in iron].

It should be noted the growth of the mineral layer in itself could slow the rate of dissolution but no correlation between the thickness of the layer and rate of carbon transfer was found.[2,4] It was argued that the change of phase to CA after a period of time densified the mineral layer making analysis of the growth (thickness) with time problematic.

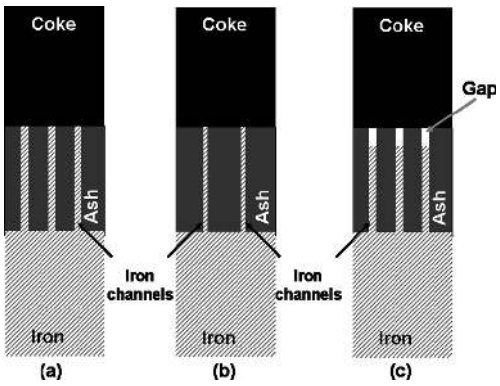

Fig. 1. Schematic of coke dissolving in iron a) after time t showing metal channels allowing the dissolution process to continue after mineral formation b) after time $t' > t$ showing fewer channels and channel narrowing resulting in a slowing of carbon transfer relative to a) and c) after time $t' > t$ showing a gap between the coke and iron stopping or slowing of carbon transfer relative to a). This gap may be a result of poor wetting/penetration characteristics of iron or side reactions between the coke–ash/mineral–iron phases resulting in a gas.

As such the effect of layer thickness has been ignored in Fig. 1.

The focus of this study was to assess the effects of interfacial wetting on the coke dissolution rate and thereby establish whether these forces could be in part responsible for inhibiting the rate of coke dissolution. Metal penetration through these channels can be described by a capillary model as given in Eq. (4)[14]

$$l \propto \frac{-r\rho g}{2\sigma \cos\theta} \quad \text{.....(4)}$$

where l, the penetration depth, is a function of the surface tension (σ) of the metal, the radius (r) of the channel, the contact angle (θ) of the iron on the mineral layer, the density (ρ) of liquid iron and gravity (g).

When l is greater than the mineral layer thickness then direct transfer can occur. There is the possibility that the mineral layer can have a thickness greater than l (as in Fig. 1(c)) and therefore prohibit direct transfer of carbon from the coke to the iron. Under such circumstances it would be expected that the rate of carbon transfer would be relatively slow as it would rely on a gas phase or reagent transfer through the mineral layer structure. If the interfacial characteristics of the CA phase in contact with liquid iron resulted in a small l relative to the mineral layer thickness, then this could be considered another possible explanation of why the coke dissolution rate slows on appearance CA in the layer. In order to assess this possibility, changes in θ of the liquid iron–mineral layer system as a result of changes in the layers mineralogy were studied and the results are reported in this paper.

2. Experimental Method

The sessile drop technique, a schematic of which is shown in **Fig. 2**, was used to measure the contact angle between iron melts and alumina, CA6, CA2 and CA mineral phases at temperatures of 1 450, 1 500 and 1 550°C. The procedure consisted of heating 0.1 ± 0.05 g of iron carbon alloy on a substrate made from the above minerals in a high purity argon atmosphere of flow rate 0.25 L/min. Using captured high definition video images, the contact angle, the droplet diameter, droplet height and contact radius were measured using the image analysis software package ImageJ with the Drop Snake plug-in. Ideally the wetting angle of the liquid should be measured in the absence of gravitational effects. Eustathopoulos[14] advises on how to calculate a critical droplet diameter that is not distorted by gravity.

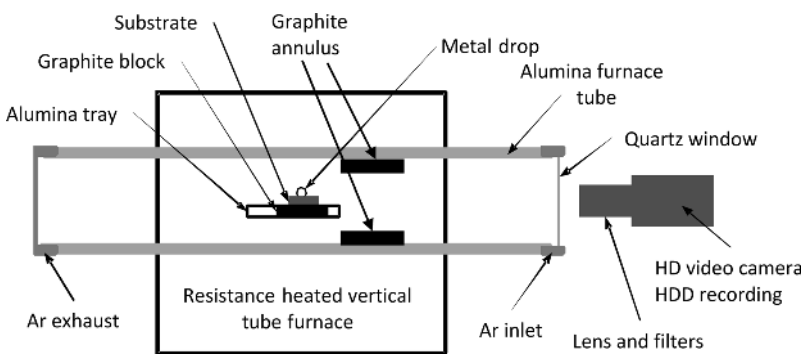

Fig. 2. A schematic showing the sessile drop furnace setup.

© 2010 ISIJ

Unfortunately this diameter is reliant on iron interfacial tension values that often have a high uncertainty associated with them. To overcome this problem and ensure the droplet diameter is much smaller than the critical diameter much smaller droplets are used but care must be taken to ensure that the image resolution error does not then dominate the wetting angle measurement. This was established experimentally and the size of droplet was selected to minimise gravitational effects (less than the critical diameter) and maximise image quality. Great care was taken to ensure that the substrate was level in the furnace.

To ensure the integrity of the iron carbon samples were not compromised as a result of oxygen entering the system the high purity argon was passed through a drierite and ascarite column then through a gettering furnace at 300°C containing Cu turnings. Further, solid graphite materials have been placed around the furnace hot zone to getter the oxygen. This included a 60 mm long graphite annulus that the inlet gas had to pass prior to reaching the sample. No measureable change in weight of these graphite materials was observed after an experiment when using a balance accurate to 0.0001 g This indicates that the furnace environment was in essence free of oxygen. Given these conditions the gas pO_2 can be predicted from the reaction

$$C\langle gr\rangle + 1/2\, O_2(g) = CO \quad \text{.....(5)}$$

Assuming an activity for graphite of 1, a pCO of 1 atm and using the thermodynamic data for reaction 5 given in Turkdogan,[15] the maximum pO_2 in the gas phase would range from 1.3×10^{-16} to 3.0×10^{-16} atm over the temperature range of 1 450 to 1 550°C.

The composition of the 2 and 5 mass% [C] melts used in the experimental programme are given in **Table 2**. These were prepared using electrolytic iron, making appropriate additions of high purity graphite (99.999+%).

Dense substrate disks were produced by pressing 3.5 to 4.0 g of finely ground (<38 μm) alumina and calcium aluminates (CA6, CA2 and CA) in a 20 mm circular steel die at a pressure of 6.5 tonnes with a moisture level of 3.5 mass%. The disks were fired in a muffle furnace in air at a temperature of 1 625°C (1 550°C for CA) for a period of 4 h then allowed to cool in the furnace. These substrates were polished to a 1 μm diamond finish prior to use in the sessile drop experiments. While it is recognised that surface roughness can have an effect on the wetting value obtained using sessile drop techniques,[14] no obvious difference in the measured wetting angle was observed when measurements were made on substrates with a 2 μm finish. The alumina and calcium aluminate phases were made from high purity alumina and $CaCO_3$ reagents and prepared in the laboratory using techniques developed by Mohamed and Sharp.[16,17] The phases were confirmed by XRD analysis. Bulk density and porosity measurements of the substrates are given in **Table 3**. These were measured in accordance with ISO 5017.[18]

Table 2. The Fe–2%[C] and Fe–5%[C] melt composition.

Melt	[C]	[S]	[Si]	[Ti]	[Mn]	[Ca]	[Al]
Fe-2%[C]	2.05	<0.003	<0.005	<0.002	<0.01	<1ppm	<0.003
Fe-5%[C]	5.01	<0.003	0.01	<0.002	<0.01	<1ppm	<0.003

A typical sessile drop image used in the θ measurement is given in **Fig. 3**, and a typical example of the stability of the wetting measurement with time is given in **Fig. 4**.

Selected wetting experiments were prepared for SEM analysis. These were cooled in the furnace under argon, an example of which is shown in **Fig. 5**. This is a SEM backscattered image and EDX map of a Fe–2%[C] on a CA substrate.

3. Results and Discussion

The contact angles for Fe–[C] melts on different substrates are given in **Fig. 6**. No attempt was made to measure the contact angle for CA at 1 550°C, as this temperature was considered too close to the CA melting temperature. From Fig. 6 it can be seen that the majority of the contact

Table 3. Density and porosity of the substrates.

Substrate	Bulk Density, g/cm^3	% Porosity
Al_2O_3	2.99	23.4
CA6	2.67	20.9
CA2	2.18	25.0
CA	2.68	10.2

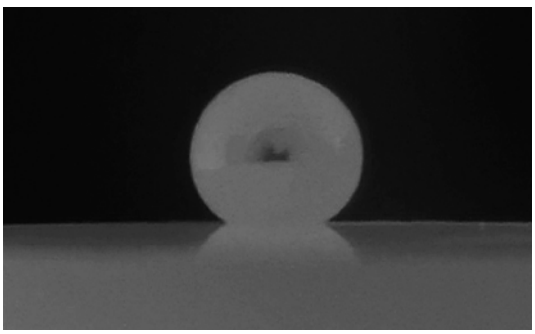

Fig. 3. Captured image of a Fe–5%[C] melt on an alumina substrate at 1 500°C. The mass of the droplet is 0.1 g.

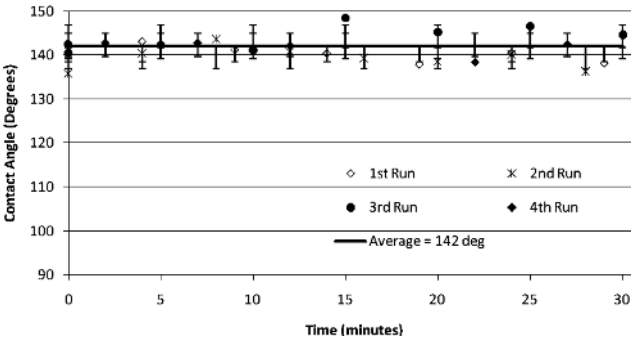

Fig. 4. The observed contact angle of the Fe–5%[C] melt on an Alumina substrate at 1 500°C. The solid line represents the average of all data shown on the plot.

© 2010 ISIJ

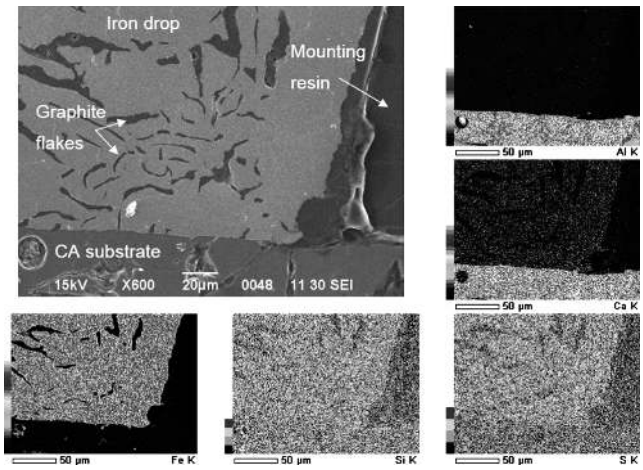

Fig. 5. A SEM backscattered image and EDX map of a Fe–2%[C] on a CA substrate after cooling in argon. The large image scale bar is 20 μm. The small images (EDX maps) the scale bar is 50 μm.

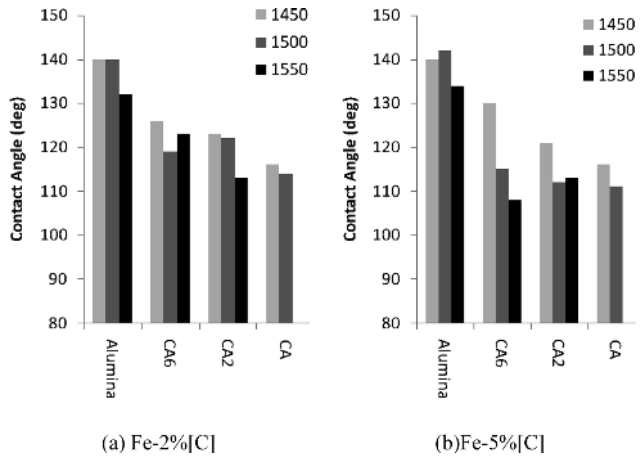

Fig. 6. Contact angle measurements for iron on alumina and calcium aluminate substrates at 1 450, 1 500 and 1 550°C with a) Fe–2%[C] and b) Fe–5%[C] droplets.

angles are between 140° to 110° and that the angle decreases as alumina→CA6→CA2→CA. This range of contact angles represents a non-wetting system that is becoming less non-wetting as the substrates change from alumina→CA6→CA2→CA. The reported contact angles are an average of the individual angles measured at approximately 5 min intervals over a 30 min period. Each combination of substrate and melt was repeated 2 or 4 times. The majority of the measurements had a scatter of less than ±5% around the mean and were time independent. The 1 550°C Fe–5%[C] melt on alumina experiments were an exception. In these experiments the contact angle tended to decrease with increasing experimental time. The decreasing contact angle indicates a dynamic wetting system. Inspection of these samples after the experimental runs indicated some reaction between the melt and alumina substrate (see **Fig. 7**). Little interaction (staining or wear of the substrate) was observed in the other samples as evidenced in Fig. 5, where no notable substrate modification was observed.

The contact angles between the iron drops and the alumina substrates measured in this study are consistent with the available literature. Values for the contact angle between pure iron and pure iron–carbon alloys and alumina are reported to be in the range of 141° to 132° in Keene's review of the system published in 1998.[19] There has been work published on pure iron on polycrystalline alumina[20] and single crystal alumina[21] since the Keene review. These are also broadly in agreement with what is report in Keene and this work. Kapilashrami *et al.*[20] measured pure iron on polycrystalline alumina at temperatures greater than 1 600°C and obtained values in the range 132° to 134°. Ueda *et al.*[21] measured pure iron on single crystal alumina and obtained values between 90 and 115° at 1 600°C. They found a significant effect of gas pO_2 on the contact angle. The higher contact angle values were at lower pO_2. This is presumably a result of the known effect of [O] on contact angles and interfacial tension. Given that the irons in this study contain significant amounts of carbon keeping the [O] low, the higher values of Ueda *et al.*[21] are more comparable with this study, though they are for pure iron. No published data was found on calcium aluminates in contact with liquid iron to make a direct comparison.

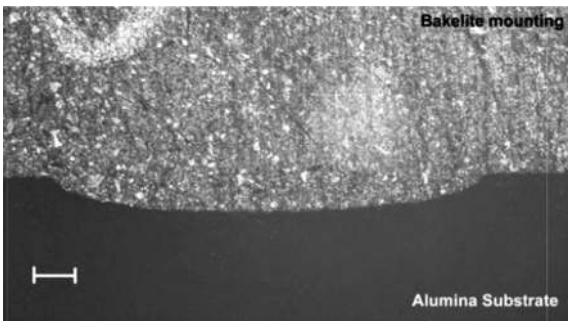

Fig. 7. Alumina substrate after reaction with C Fe–5%[C] at 1 550°C. The scale bar is 250 μm. The iron droplet was not adhered to the substrate when mounting this sample.

3.1. Potential Metal–Substrate Interactions

At 1 550°C, the apparent time dependence of the contact angle in the Fe–5%[C] melt on an alumina substrate, and the depression shown in Fig. 7, indicates that there is a reaction occurring between the substrate and the melt. The most likely reaction would be that involving alumina and the solute carbon in the melt. Though such a reaction is not normally considered thermodynamically favoured other workers have made similar observations with iron and alumina at this temperature.

In surface tension studies Kozakevitch and Urbain[22] observed reaction between high carbon alloys and alumina at 1 550°C, and suggested that bubbles of CO were formed at the interface. They also noted that the intensity of this reaction was decreased at 1 500°C. Nizhenko and Floka[23] observed bubbles at the melt interface of Fe–C melts of eutectic composition and alumina at 1 600°C, noting a significant increase of the aluminium content of the melt. As a result of these studies Keene's review of iron surface tension data he warns that high carbon Fe–C[24] surface tension data "should be treated with caution". Though little interaction between the liquid iron melts and the substrates was observed in this study for the majority of the wetting measurements Keene's warning may also be applicable, particularly to the 1 550°C Fe–5%[C] melts.

© 2010 ISIJ

3.2. Effect of Temperature on Contact Angle

Within the Fe–C melt results, an increase in temperature results in a lowering of the contact angle of the melt on the alumina and calcium aluminate substrates. This indicates an increase in the wetting of the substrate. This is consistent with the expected decrease in the surface tension of the melt with increased temperature; however it may also represent the increased substrate interaction with the droplet.

3.3. Effect of Substrate on Contact Angle

The different calcium aluminates display different wetting behaviour from alumina and each other. It was found that the contact angle decreased (the wetting increased) as the proportion of lime (CaO) in the substrate was increased. The data for 1 450°C in Fig. 6 have been re-plotted in **Fig. 8** to demonstrate this trend. Data from the literature of iron wetting on Al_2O_3 and CaO[17] substrates are included as vertical bars spanning the reported range of contact angles.

3.4. Effect of Carbon Content on the Contact Angle

The contact angles between the two different Fe–C melts on the substrates is similar and within the ±5% scatter reported for the results, the exception being the 1 550°C CA6 data. Tsarevskii and Popel[25] found that there was only a small decrease in the wetting angle of approximately 3° over a composition change of 2 to 5% [C]. Such a small difference is consistent with the majority of contact angles measured in this study, with respect to changes in [%C], and indicate that the carbon level has only a very minor effect on the contact angle. The discrepancy in the values using the 2 and 5% [C] melts on CA6 at 1 550°C, is more likely to be caused by the influence of substrate interactions not identified in this study. This is likely to form the basis of a future investigation.

3.5. Contact Angle, Wetting and Coke Dissolution in Iron

The substrate–liquid iron contact angles measured in this study (Fig. 6) are indicative of a non wetting system, though the system is becoming less non-wetting as the substrates are changed from alumina→CA6→CA2→CA. For all other things being equal, and considering Eq. (4), a lower contact angle (greater wetting) would result in a greater depth of penetration of the mineral layer. Therefore from the contact angles measured there is a greater potential for the melt to penetrate a mineral layer formed on coke dissolution as the mineral layer changes from alumina→CA6→CA2→CA. If this was the sole parameter that affected coke dissolution in iron it would be expected that as the layer progressively became enriched in calcium oxide a thicker layer could be tolerated before the layer thickness exceeded *l*, the penetration depth in Eq. (4), and stopped coke dissolution. It has been reported that the rate of carbon transfer into iron slowed on appearance of CA.[2] It was argued that this was due to densification of the mineral layer at the coke–iron interface as a result of CA formation. In the aforementioned study no distinction could be made between mechanisms coke dissolution slowing mechanisms represented Figs. 1(b) and 1(c). The contact angle/wetting data presented here eliminate the changing wetting characteristics as depicted in Fig. 1(c) as a cause of slowing down the coke dissolution reaction. Since the wetting increases as CA6→CA2→CA, CA formation would either have a neutral or positive effect on the rate of carbon transfer/coke dissolution.

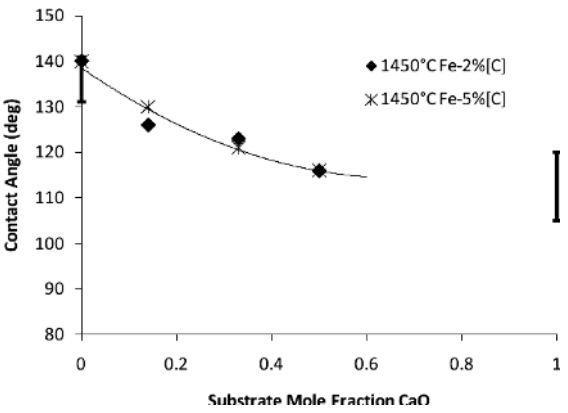

Fig. 8. The influence of substrate on contact angle at 1 450°C.

4. Conclusions

The wetting behaviour of two iron carbon alloys (2 and 5 mass% [C]) have been measured at 1 450, 1 500 and 1 550°C at on substrates of alumina, CA6, CA2, and CA. The systems were in general non-wetting, the contact angle ranging from approximately 140° to 110° as the substrates change from alumina→CA6→CA2→CA. Moreover these results have been used to eliminate changes in interfacial wetting as a result of mineral layer composition changes as a cause for slowing down the rate of coke dissolution in iron.

The effects of temperature and [%C] on the contact angle were measured over a temperature range of 1 450 to 1 550°C and 2 and 5 mass% [C] though no strong correlation was found. At 1 550°C there was some evidence of reaction with iron and the alumina substrate for the 5 mass% [C]. This was considered unusual but has been reported by other researchers and discussed in terms of alumina reduction.

Acknowledgement

The authors would like to thank Drs. John Mathieson and Robert Nightingale of BlueScope Steel Ltd. and the Australian Research Council for supporting this research.

REFERENCES

1) Y. E. Omori Ed.: Blast Furnace Phenomena and Modelling, Elsevier Applied Science, London, (1987), 58.
2) M. W. Chapman, B. J. Monaghan, S. A. Nightingale, R. J. Nightingale and J. G. Mathieson: *Metall. Mater. Trans. B*, **39B** (2008), 418.
3) B. J. Monaghan, M. W. Chapman, S. A. Nightingale, R. J. Nightingale and J. G. Mathieson: Scanmet III, Vol. 2, Lulea, Sweden, (2008), 135.
4) M. W. Chapman, B. J. Monaghan, S. A. Nightingale, R. J. Nightingale and J. G. Mathieson: Scanmet III, Vol. 2, Lulea, Sweden, (2008), 245.
5) R Kiessling and N Lange: Non Metallic Inclusions in Steel, Vol. 2, The Metals Society, London, (1978), 36.
6) M. Kowalski, P. J. Spencer and D. Neuschutz. Phase Diagrams, VDE (VDEh), ed. Slag Atlas, Dusseldorf, Verlag Stahleisen GmbH, (1995), 39.

© 2010 ISIJ

7) H. W. Gudenau, J. P. Mulanza and D. G. R. Sharma: *Steel Res.*, **61** (1990), 97.
8) S. Orsten and F. Oeters: Process Technology Proc., Iron and Steel Society, Washington D.C, (1986), 143.
9) F. McCarthy, R. Khanna, V. Sahajwalla and N. Simento: *Iron Steel Inst. Jpn. Int.*, **45** (2005), 1261.
10) F. McCarthy, V. Sahajwalla, J. Hart and N. Saha-Chaudhury: *Metall. Trans. B*, **34B** (2003), 573.
11) R. Khanna, F. McCarthy, H. Sun, N. Simento and V. Sahajwalla: *Metall. Trans. B*, **36B** (2005), 719.
12) M. W. Chapman, B. J. Monaghan, S. A. Nightingale, R. J. Nightingale and J. G. Mathieson: Australia–China–Japan Symposium on Iron and Steelmaking, Liaoning Science and Technology Publishing House, China, (2006), 90.
13) M. W. Chapman, B. J. Monaghan, S. A. Nightingale, R. J. Nightingale and J. G. Mathieson: *Iron Steel Inst. Jpn. Int.*, (2007), 973.
14) N. Eustathopoulos, M.G. Nicholas and B. Drevet: Wettability at High Temperatures, 1st ed., Pergamon Materials Series, ed. by R. W. Cahn, Oxford, Elsevier Science, (1999).
15) E. T. Turkdogan: Fundamentals of Steelmaking, The Institute of Metals, London, (1996), 10.
16) B. M. Mohamed and J. H. Sharp: *J. Mater. Chem.*, **7** (1997), 1595.
17) B. M. Mohamed and J. H. Sharp: *Thermochim. Acta*, **388** (2002), 105.
18) ISO, ISO 5017 Dense Shaped Refractor Products—Determination of Bulk Density, Apparent Porosity and True Porosity, (1998).
19) B. J. Keene: Contact Angle and Work of Adhesion between Ferrous Melts and Non-metallic Solids, Slag Atlas 2nd ed., Duesseldorf, Verlag Sthleisen GmbH, (1995), 513.
20) E. Kapilashrami, A. Jakobsson, A. K. Lahiri and S. Seetharaman: *Metall. Mater. Trans. B*, **34** (2003), 193.
21) S. Ueda, H. Shi, X. Jiang, H. Shibata and A. W. Cramb: *Metall. Mater. Trans. B*, **34** (2003), 503.
22) P. Kozakevitch and G. Urbain: *Mem. Sci. Rev. Metal.*, **58** (1961), 401.
23) V. Nizhenko and L. Floka: *Powder Metall. Met. Ceram.*, **10** (1972), 819.
24) B. J. Keene: *Int. Mater. Rev.*, **33** (1988), 1.
25) B. V. Tsarevskii and S. I. Popel: *Vuz. Chern. Metall.*, **8** (1960), 15.

© 2010 ISIJ